

## Contact interface fiber section element: shallow foundation modeling

Suchart Limkatanyu\*<sup>1</sup>, Minh Kwon<sup>2</sup>, Woraphot Prachasaree<sup>1</sup>  
and Passagorn Chaiviriyawong<sup>1</sup>

<sup>1</sup>*Department of Civil Engineering, Faculty of Engineering, Prince of Songkla University,  
Songkhla 90112, Thailand*

<sup>2</sup>*Department of Civil Engineering, ERI, Gyeongsang National University, Jinju, South Korea*

*(Received August 11, 2011, Revised May 30, 2012, Accepted June 15, 2012)*

**Abstract.** With recent growing interests in the Performance-Based Seismic Design and Assessment Methodology, more realistic modeling of a structural system is deemed essential in analyzing, designing, and evaluating both newly constructed and existing buildings under seismic events. Consequently, a shallow foundation element becomes an essential constituent in the implementation of this seismic design and assessment methodology. In this paper, a contact interface fiber section element is presented for use in modeling soil-shallow foundation systems. The assumption of a rigid footing on a Winkler-based soil rests simply on the Euler-Bernoulli's hypothesis on sectional kinematics. Fiber section discretization is employed to represent the contact interface sectional response. The hyperbolic function provides an adequate means of representing the stress-deformation behavior of each soil fiber. The element is simple but efficient in representing salient features of the soil-shallow foundation system (sliding, settling, and rocking). Two experimental results from centrifuge-scale and full-scale cyclic loading tests on shallow foundations are used to illustrate the model characteristics and verify the accuracy of the model. Based on this comprehensive model validation, it is observed that the model performs quite satisfactorily. It resembles reasonably well the experimental results in terms of moment, shear, settlement, and rotation demands. The hysteretic behavior of moment-rotation responses and the rotation-settlement feature are also captured well by the model.

**Keywords:** fiber-section model; shallow foundation element; soil-structure interaction; winkler foundation; soil bearing capacity; rocking foundation; contact-interface element; nonlinear analysis.

---

### 1. Introduction

The interaction problem between a shallow foundation and its contacting soils has been a key challenge to structural and geotechnical engineers in analyzing, designing, and evaluating both newly constructed and existing buildings under seismic events. Generally, this soil-structure interaction problem involves two complex nonlinear phenomena, namely: material nonlinearity and geometric nonlinearity. The former is related to yielding of the contacting soils as well as gap formation at soil-foundation interfaces while the latter is related to the foundation uplift. These two sources of

---

\*Corresponding author, Associate Professor, E-mail: [suchart.l@psu.ac.th](mailto:suchart.l@psu.ac.th)

nonlinearities render shallow foundations to slide, settle, and rock under seismic loadings (Yang *et al.* 2000). Consequently, inclusion of these three interaction mechanisms (sliding, settling, and rocking) into a foundation numerical model is important for design, analysis, and performance evaluation of structures under seismic actions. This is especially true when the Performance-Based Seismic Design and Assessment Methodology (SEAOC. Vision 2000, 1995) is adopted. In this design and assessment methodology, it urges structural and geotechnical engineers to utilize the beneficial effects from the nonlinear soil-structure interaction to reduce the structural force and ductility demands. These beneficial effects are generally resulted from mobilization of the foundation ultimate capacity and its interaction mechanisms for dissipating seismic energy. However, the inherent detrimental effects from mobilization of the foundation ultimate capacity (e.g., permanent settlement, permanent tilt, induced secondary moment, etc.) have to be taken into account. Consequently, the nonlinear shallow foundation model capable of considering both beneficial and detrimental interaction effects is a vital element in implementations of the recently proposed Performance-Based Seismic Design and Assessment Methodology.

Several mathematical models with various degrees of complexity have been developed in the literature to represent the interaction mechanisms between shallow foundations and contacting soils. These models can be categorized into three groups, namely: (a) continuum finite element model; (b) discrete Winkler-based spring model; and (c) macro-element model. Some recent examples and applications of the continuum finite element model developed for the analysis of soil-shallow foundation systems are found in Huat and Mohammed (2006) and Burnier *et al.* (2007). In the continuum finite element model, a semi-infinite soil medium is discretized by continuum finite elements and the effects of inhomogeneous soil mass can be accounted for automatically. Analyses performed with continuum finite elements provide comprehensive details but are hampered by high computational costs. Therefore, only foundation components or small structural systems can be realistically investigated using the continuum finite element models. On the other hand, the Winkler-based spring model and the macro-element model have been employed by several researchers as alternative less-expensive and/or less time consuming means to study the soil-shallow foundation interaction problems.

In the Winkler-based spring model as discussed in the classical textbook by Scott (1981), a set of 1-D independent soil springs are attached along the beam element to form the soil-shallow foundation system. The force-deformation characteristics of the soil springs are usually calibrated such that they can represent the salient features of the soil-shallow foundation system observed during the tests. An early effort on using the Winkler-based spring approach to capture the rocking mechanism of shallow foundations was put forward by Taylor *et al.* (1981). Subsequent notable studies on the Winkler-based shallow foundation models were contributed by several researchers. For examples, Chopra and Yim (1985) developed the Winkler-based shallow foundation model with elastic-plastic soil springs to account for the beneficial effects of foundation rocking and uplifting on the base shear for stiff (short-period) structures. Nakaki and Hart (1987) used the Winkler-based shallow foundation model with elastic contact-breaking soil springs to study the inelastic responses of shear walls and observed that the ductility demands were greatly reduced due to the uplifting of foundation bases, especially for stiff shear walls. Using the geotechnical centrifuge (75 g centrifugal acceleration) at the University of California, Davis (UC-Davis), several researchers have performed excellently both experimental and analytical studies on soil-shallow foundation interaction problems. Rosebrook (2001) and Gajan (2006) conducted several series of tests on a prototype shear wall footing at 20 g centrifugal acceleration. Ugalde (2007) performed a series of centrifuge tests at

42.9 g centrifugal acceleration on bridge columns on shallow square footings. Calibrating with the aforementioned experimental results, Raychowdhury (2008) developed the Winkler-based soil spring models to simulate the soil-shallow foundation interaction effects. Even though the Winkler-based spring models proposed by the abovementioned researchers are simple but efficient to represent the salient features of soil-shallow foundation systems, there are two inherent drawbacks that need to be mentioned when dealing with the rigid-footing assumption. Firstly, several beam nodes are needed in order to connect the beam with the soil springs, resulting in unnecessary degrees of freedom (DOFs). Secondly, a large value of flexural rigidity is needed to emulate the rigid-footing response. This could lead to the problem of numerical instability. An alternative way to cope with the rigid-footing assumption is to use the multi-point constraint technique. However, this constraint feature may not be easily available in a general structural-analysis platform.

In the macro-element model, the entire soil-shallow foundation system is simply represented by a single joint element located at the base of the superstructure. Therefore, there are 3 DOFs for a 2-D case and 6 DOFs for a 3-D case. The plastic yield surface and plastic potential function are used to describe the resultant force-displacement behavior of the element. The first macro-element model was developed by Nova and Montrasio (1991) to evaluate displacements of strip footings on sand. An isotropic hardening rigid-plastic law was used as the constitutive law of this model. Houlsby and Cassidy (2002) also developed a macro-element model based on the work-hardening plasticity theory to study the behavior of circular footings on sand. These two macro-element models are applicable to sand but are limited only to monotonic loadings. The first macro-element model capable of describing the cyclic behavior of footings was proposed by Paolucci (1997). Only material nonlinearity due to soil yielding was considered in the model using an isotropic-hardening elasto-plastic law. Cremer *et al.* (2001) enhanced the macro-element model of Paolucci (1997) by incorporating geometric nonlinearity due to foundation uplift into the model. Following pioneering studies by Paolucci (1997) and Cremer *et al.* (2001), several improved macro-element models have been developed by several researchers (e.g., Gajan 2006, Shirato *et al.* 2008, Grange *et al.* 2008, Chatzigogos *et al.* 2011). Even though the aforementioned macro-element models can fully account for the coupling effects between all force components (horizontal force, vertical force, and moment), two inherent difficulties need to be pointed out. Firstly, large numbers of material parameters are generally needed to be input by users. Secondly, the model implementation typically requires an extensive effort. These could limit the model access by practicing engineers.

The main objective of this paper is to propose a simplified but efficient contact interface element for modeling soil-shallow foundation systems. The contact interface constitutive model stems from the fiber section discretization approach widely used in describing sectional responses of reinforced concrete and steel members (Spacone *et al.* 1994). Each fiber in the fiber section model represents the contacting soil. The assumption of a rigid footing on the Winkler-based soil rests on the Euler-Bernoulli's hypothesis on sectional kinematics. In the Euler-Bernoulli's beam theory, it is assumed that the beam section remains plane and normal to the beam axis after experiencing the flexural deformation. This hypothesis corresponds to the kinematics of the rigid footing. The contact interface element proposed here can be categorized as a mixture of Winkler-based spring and macro-element models. It combines desirable features of both the Winkler-based spring and the macro-element models. Therefore, it can easier be implemented in a general structural-analysis platform and accessed by practicing engineers. Two experimental results are used to illustrate the model characteristics and verify the model accuracy. All salient interaction mechanisms (settling, uplifting, rocking, and sliding) are reasonably represented by the proposed model. The general-purpose finite element

program FEAP (Taylor 2000) is used to host the proposed element.

**2. Definition**

In the present work, the contact interface fiber section (CIFS) element shown in Fig. 1(a) is proposed to model the responses of shallow foundations. The element has two nodes connected by a zero-length contact interface section. The zero-length contact interface section is used to represent the interaction mechanics between the footings and the contacting soils. The idealization of the superstructure-footing system is shown in Fig. 1(b).

Following the notation of Fig. 1(a), the element nodal displacements are

$$\mathbf{U} = \{\mathbf{U}^1; \mathbf{U}^2\}^T \tag{1}$$

where  $\mathbf{U}^1 = \{U_1 \ U_2\}^T$  and  $\mathbf{U}^2 = \{U_3 \ U_4\}^T$  are arrays containing the displacements at nodes 1 and 2, respectively. Their work-conjugate nodal forces are grouped in the element force vector  $\mathbf{P} = \{\mathbf{P}^1; \mathbf{P}^2\}^T$ .

The contact interface sectional deformations comprise of the axial deformation  $u$  and transverse rotation  $\theta$  and are grouped in the following array

$$\mathbf{d} = \{u \ \theta\}^T \tag{2}$$

The corresponding contact interface sectional forces  $\mathbf{D}$  are

$$\mathbf{D} = \{N \ M\}^T \tag{3}$$

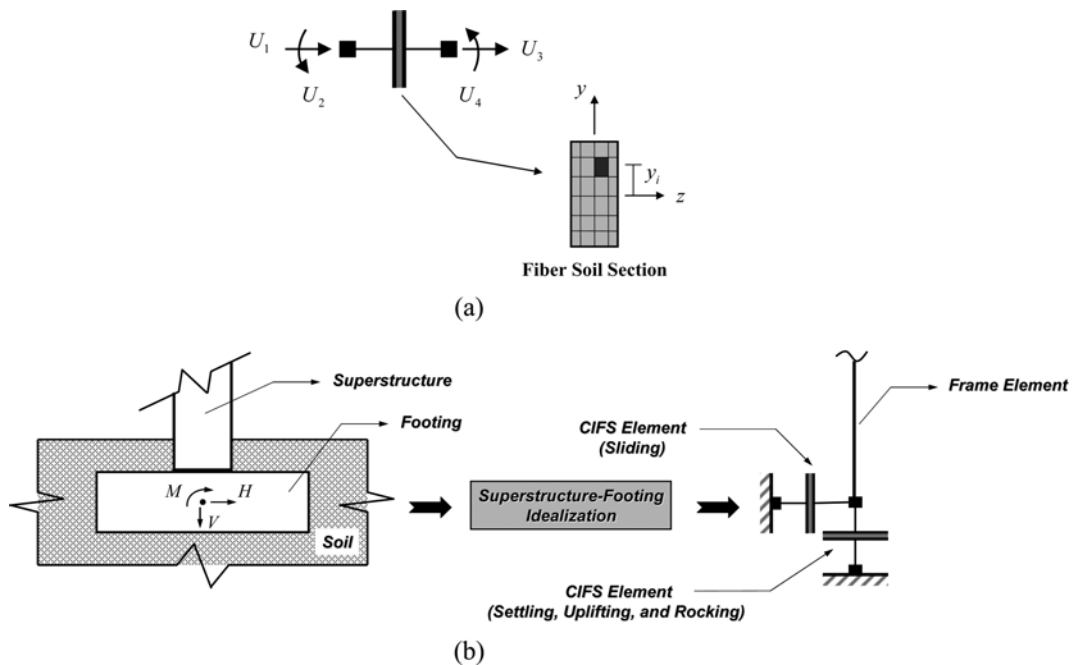


Fig. 1 (a) Contact interface fiber section (CIFS) element; (b) Superstructure-footing idealization

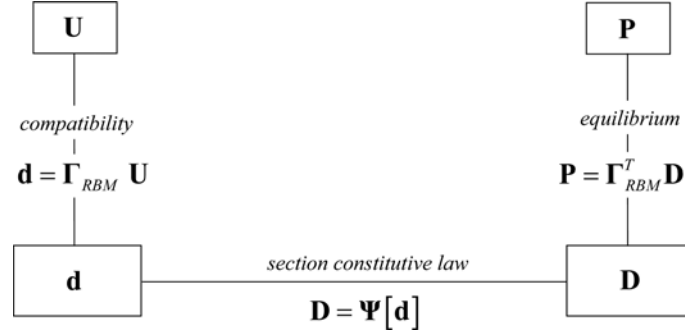


Fig. 2 Tonti's diagram for contact interface fiber section element

where  $N$  and  $M$  are the axial force and the bending moment, respectively.

### 3. Contact interface fiber section element: formulation

Three sets of governing equations describing the proposed contact interface foundation element are compatibility, contact interface section constitutive equations, and equilibrium. The so-called “Tonti's diagram” of Fig. 2 is used to conveniently represent these governing equations.

#### 3.1 Compatibility

Considering the element kinematics, the contact interface sectional deformations  $\mathbf{d}$  are related to the element nodal displacements  $\mathbf{U}$  through the following equations

$$\mathbf{d} = \Gamma_{RBM} \mathbf{U} \quad (4)$$

where  $\Gamma_{RBM}$  is the rigid-body mode transformation matrix, defined as

$$\Gamma_{RBM} = \begin{bmatrix} -1 & 0 & 1 & 0 \\ 0 & -1 & 0 & 1 \end{bmatrix} \quad (5)$$

#### 3.2 Contact interface constitutive laws: fiber section discretization

The contact interface sectional forces  $\mathbf{D}$  and deformations  $\mathbf{d}$  are related through a nonlinear deformation-based constitutive model

$$\mathbf{D} = \Psi [\mathbf{d}] \quad (6)$$

In the present work, the fiber section model with nonlinear uniaxial stress-deformation laws for the contacting soil is used to derive and linearize the nonlinear function in Eq. (6). The contact interface section is subdivided into fibers. Based on application of virtual displacement principle, the contact interface forces  $\mathbf{D}$  are

$$\mathbf{D} = \sum_{j=1}^{nfib} \{ \sigma_j A_j - y_j \sigma_j A_j \}^T \quad (7)$$

where  $j$  represents the generic soil fiber and  $nfib$  is the number of soil fibers in the contact interface section.  $y_j$ ,  $\sigma_j$ , and  $A_j$  are the distance from the reference axis (Fig. 1), the soil stress, and the area, respectively, of soil fiber  $j$  of the contact interface section. The soil stress  $\sigma_j$  can represent bearing pressure  $q_j$  and frictional shear stress  $t_j$  depending on its interaction mechanism. It is noted that the kinematics of the contact interface section follows the Euler-Bernoulli beam theory, thus leading to the rigid-footing assumption.

The contact interface section stiffness  $\mathbf{k}$  is

$$\mathbf{k} = \sum_{j=1}^{nfib} \begin{bmatrix} E_j A_j & -y_j E_j A_j \\ -y_j E_j A_j & y_j^2 E_j A_j \end{bmatrix} \quad (8)$$

where  $E_j$  is the soil fiber modulus. Therefore, the nonlinear force-deformation relation for the contact interface section can be written in a consistent linearized matrix form as

$$\mathbf{D} = \mathbf{D}^0 + \mathbf{k} \Delta \mathbf{d}^0 \quad (9)$$

where  $\mathbf{D}^0$  is the initial contact interface section forces.

### 3.3. Equilibrium: the virtual displacement principle

The equilibrium relation between the contact interface forces  $\mathbf{D}$  and the element nodal forces  $\mathbf{P}$  can be obtained using the invariant property of virtual work. Substituting Eq. (4) and subsequently imposing the arbitrariness of the virtual nodal displacements  $\delta \mathbf{U}$  result in the following equilibrium relation

$$\Gamma_{RBM}^T \mathbf{D} = \mathbf{P} \quad (10)$$

Substitution of Eqs. (9) into (10) yields the incremental form of equilibrium as

$$\mathbf{K} \Delta \mathbf{U} = \mathbf{P} - \mathbf{P}^0 \quad (11)$$

where  $\mathbf{K} = \Gamma_{RBM}^T \mathbf{k} \Gamma_{RBM}$  is the shallow foundation element stiffness matrix; and  $\mathbf{P}^0 = \Gamma_{RBM}^T \mathbf{D}^0$  is the element resistant force vector.

## 4. Contact interface sectional constitutive laws

The contact interface fiber section element proposed in this work can be used to model three interaction modes between shallow foundations and surrounding soils, namely: sliding, settling, and rocking. The vertical bearing response of underlying soils is required to model the settling and rocking interaction modes and is represented by the so-called “ $q$ - $z$  element”. The shear-friction response of surrounding soils is needed to represent the sliding interaction mode and is modeled by the so-called “ $t$ - $x$  element”. Fig. 3 shows a schematic arrangement of these two elements to represent the sliding, settling, and rocking interaction modes. Constitutive laws of surrounding soils

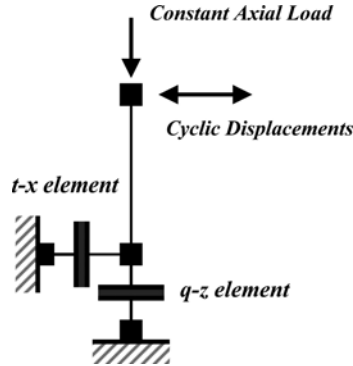


Fig. 3 Schematic arrangement of the  $q$ - $z$  and  $t$ - $x$  elements

for the  $q$ - $z$  and  $t$ - $x$  elements are described as follows

#### 4.1. Vertical bearing response of underlying soils: $q$ - $z$ curve

In this study, the soils underneath a footing are represented by 1-D springs continuously distributed within the footing area. The so-called “ $q$ - $z$  curve” is used to characterize these 1-D soil springs. Several researchers (e.g., Terzaghi 1943, Meyerhof 1963, Hansen 1970, etc.) have proposed different formulae to compute the ultimate vertical bearing pressure. In this study, the ultimate vertical bearing formula proposed by Meyerhof (1963) is employed since it is widely used by geotechnical engineers (Cernica 1995). Based on the formulae proposed by Meyerhof (1963), the ultimate vertical bearing pressure  $q_{ult}$  is defined as

$$q_{ult} = cN_c s_c d_c i_c + \bar{q}N_q s_q d_q i_q + 0.5\gamma B N_\gamma s_\gamma d_\gamma i_\gamma \quad (12)$$

where  $c$  is the soil cohesion;  $\bar{q}$  is the effective overburden pressure at base level;  $\gamma$  is the soil effective unit weight;  $B$  is the footing width;  $N_c$ ,  $N_q$ , and  $N_\gamma$  are the bearing capacity factors;  $s_c$ ,  $s_q$ , and  $s_\gamma$  are the shape factors;  $d_c$ ,  $d_q$ , and  $d_\gamma$  are the depth factors; and  $i_c$ ,  $i_q$ , and  $i_\gamma$  are the inclination factors. The explicit expressions of these factors can be found in most foundation engineering textbooks (e.g. Cernica 1995).

The monotonic  $q$ - $z$  curve of underlying soils is shown in Fig. 4(a). The response curve between the bearing soil pressure  $q$  and soil settlement  $z$  is described by a general hyperbolic equation proposed by Duncan and Chang (1970) and Duncan and Mokwa (2001) as

$$q = \frac{z}{\left( \frac{1}{k_{vmax}} + R_f \frac{z}{q_{ult}} \right)} \quad (13)$$

where  $k_{vmax}$  is the initial stiffness of the  $q$ - $z$  response curve and  $R_f$  is the failure ratio and serves as a reduction factor to remedy the overestimation of the soil strength inherent in the general hyperbolic function. The value of  $k_{vmax}$  can be calculated using the elastic formulae proposed by Gazetas (1991). These formulae have been adopted in several seismic design and rehabilitation documents (e.g. ATC-40 1996, FEMA-273 1997, etc.). As recommended by ATC-40 (1996), the contact interface section is divided into two regions, namely: end region and middle region. The end-region

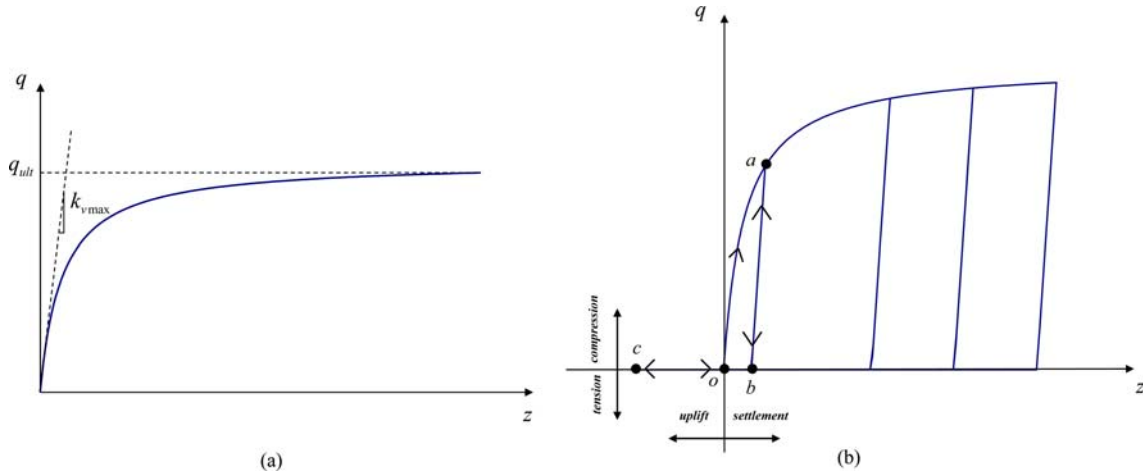


Fig. 4 Hyperbolic  $q$ - $z$  model: (a) monotonic response; (b) cyclic response

initial stiffness  $k_{vmax}^{end}$  is derived from the vertical stiffness for a rigid plate of the size  $B \times \frac{B}{6}$  while the middle-region initial stiffness  $k_{vmax}^{middle}$  is based on that for an infinitely long rigid plate. The value of  $k_{vmax}^{end}$  is approximately nine times that of  $k_{vmax}^{middle}$ . This non-uniform distribution of initial stiffness accounts for the fact that the soil within an end region is compressed more than that within a middle region during rocking mechanism, thus increasing vertical soil stiffness due to densification. The failure ratio  $R_f$  is related to the hyperbolic asymptotic value of the ultimate vertical bearing pressure. As suggested by Duncan and Chang (1970), the value of  $R_f$  generally ranges from 0.75 to 0.95. A value of  $R_f = 0.8$  is adopted in this study since it leads to satisfactory responses when compared with those obtained by the more refined  $q$ - $z$  spring model implemented in OpenSees (2008). Fig. 4(b) exemplifies the cyclic response of the  $q$ - $z$  model. A schematic representation of the hysteretic laws is explained as follows. Referring to Fig. 4(b), the soil is loaded first along the monotonic branch  $oa$  and then is elastically unloaded with the initial stiffness until the soil bearing pressure completely vanishes at  $b$ . From points  $b$  to  $c$ , the soil spring is inactivated when it moves through the gap along the branch  $bo$  and experiences the uplifting response along the branch  $oc$ . The soil spring is reactivated when the gap is closed at point  $b$  and experiences the reloading response along the branch  $ba$ .

#### 4.2 Frictional resistant response of underlying soil-footing interfaces: $t$ - $x$ curve

In this study, the frictional sliding resistance along the underlying soil-footing interface is represented by 1-D springs distributed within the contact interface section. The so-called “ $t$ - $x$  curve” is used to characterize these 1-D interface springs. Based on the classical Mohr-Coulomb failure criteria, the ultimate sliding shear strength  $t_{ult}$  can be computed as

$$t_{ult} = \frac{W_{structure}}{A_{footing}} \tan \delta + c \tag{14}$$

where  $W_{structure}$  is the structural weight transferred to the considered footing;  $A_{footing}$  is the footing

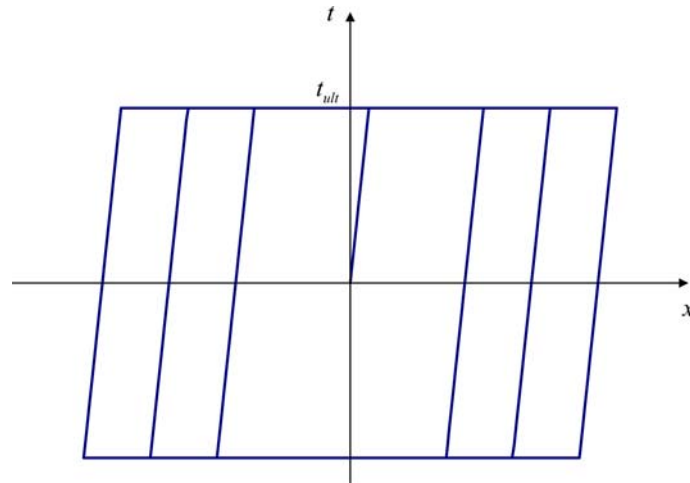


Fig. 5 Elastic-perfectly plastic  $t$ - $x$  model

surface area; and  $\delta$  is the frictional angle between the underlying soil-footing interfaces. Based on a series of interface shear tests on a variety of construction materials and soils, Potyondy (1961) provided conservative estimates of  $\delta$ . As a rule of thumb, a value of  $\delta$  ranging from  $\phi/3$  to  $2\phi/3$  is commonly used by practicing geotechnical engineers (Raychowdhury 2008).

The elastic-perfectly plastic hysteretic model is used to characterize the cyclic response of the  $t$ - $x$  curve as shown in Fig. 5. A large value of initial stiffness is used to reconcile the rigid-plastic behavior of the frictional-sliding resisting mechanism.

## 5. Model validation against experimental results

The results from two experimental tests are used to verify the accuracy of the models. The first one is a shearwall strip footing on stiff clay cyclically tested in the 9.1  $m$ -radius beam centrifuge at the University of California, Davis. This experimental set is used to verify the model ability to represent the sinking-dominated foundation response. The second one is a 1- $g$  experiment of a square footing on dense sand under cyclic loadings tested at the ELSA laboratory in Italy and is employed to show the model capability of simulating the rocking-dominated foundation response.

### 5.1 UC-Davis centrifuge experiment: KKR-03

At UC-Davis, Rosebrook (2001) conducted three series of centrifugal tests at 20  $g$  centrifugal acceleration to investigate the nonlinear behavior of shearwall strip footings under vertical push, lateral cyclic loadings, and base excitations. KKR-01 and KKR-02 were first two series conducted on dry sand ( $D_r \approx 80\%$  and  $60\%$ ) while KKR-03 was the last series conducted on stiff consolidated clay. The experimental results of KKR-03 test series under lateral cyclic loadings are used to validate the proposed shallow foundation model.

Fig. 6 shows the centrifuge test setup for KKR-03 model under lateral cyclic loadings. The structure consists of a 10  $m$ -high double shearwall system and has a weight of 365  $kN$ . This value

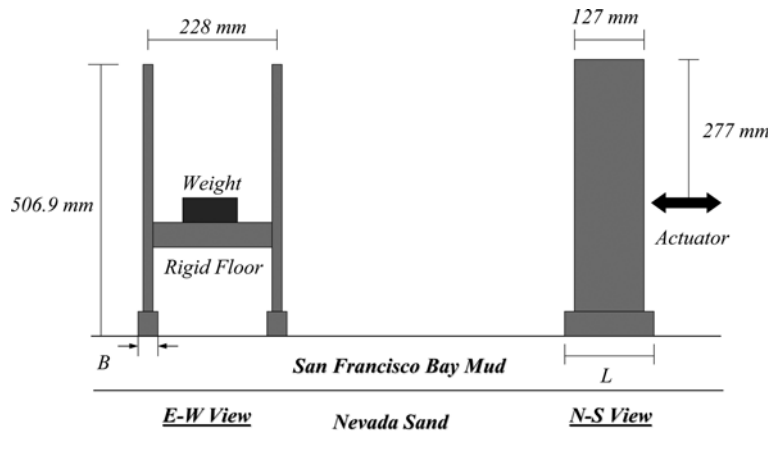


Fig. 6 Test setup of KKR-03 experiment (After Gajan 2006)

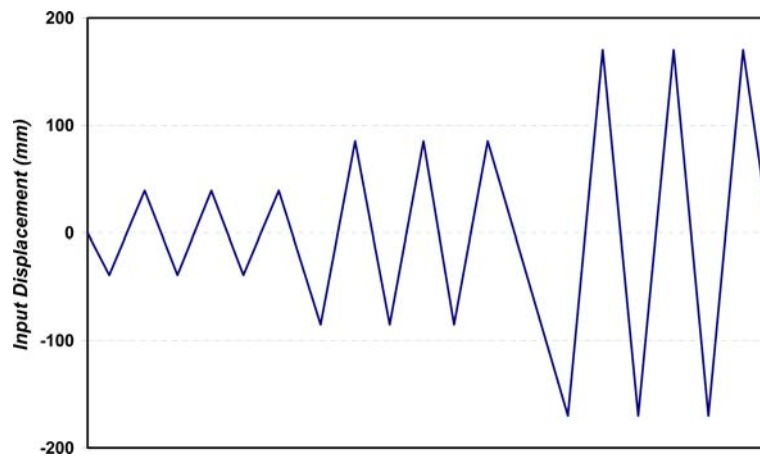
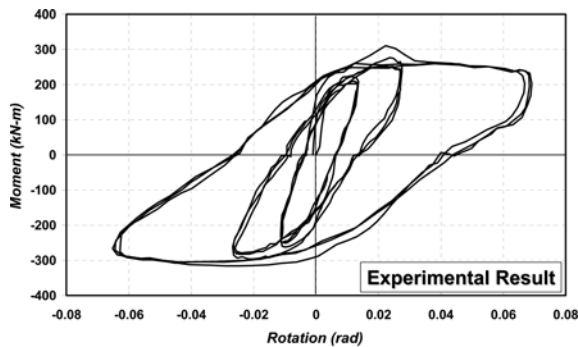


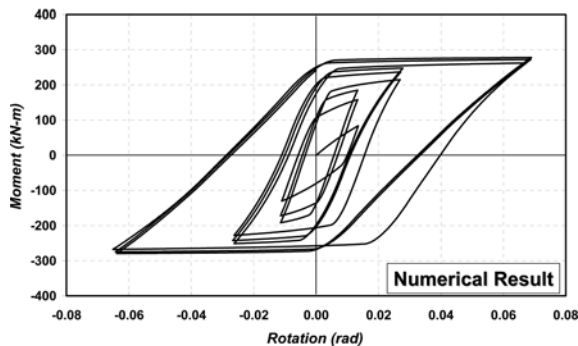
Fig. 7 Imposed displacement history of KKR-03 experiment

of structural weight results in a static vertical factor of safety  $FS_V \approx 2.8$ . The strip footing has the size of  $B = 0.69 \text{ m} \times L = 2.67 \text{ m}$  and rests on the 1.7 m-thick stiff clay layer remolded from San Francisco Bay Mud with an average value of undrained shear strength of 103 kPa. After subjecting to a concentric vertical push, a set of cyclic displacements shown in Fig. 7 are applied via an actuator at a height of 4.75 m from the footing base. The set of imposed cyclic displacements is composed of three packets of increasing amplitude. Each packet contains three cycles of a symmetric reversed loading with constant amplitude. It is noted that all aforementioned dimensions are in the prototype scale.

Due to symmetry, only half of the double shearwall system is modeled as shown in Fig 3. The shearwall is modeled with a conventional frame element. Axial and flexural deformations of the shearwall are neglected using large values of axial and flexural rigidities. The proposed  $q$ - $z$  and  $t$ - $x$  contact interface elements are used to represent the soil-footing interaction mechanisms. Eighty soil fibers are used to discretize the  $q$ - $z$  contact interface section while only one soil fiber is used for the

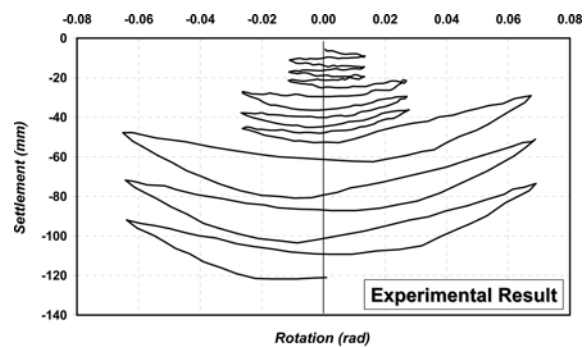


(a)

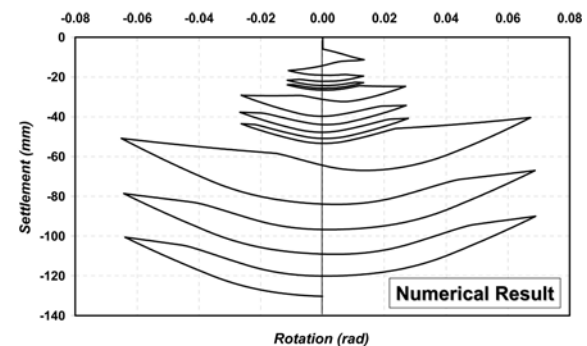


(b)

Fig. 8 Experimental and numerical moment-rotation responses of KKR-03 experiment



(a)



(b)

Fig. 9 Experimental and numerical settlement-rotation responses of KKR-03 experiment

$t$ - $x$  contact interface section. The elastic modulus  $E$  and Poisson ratio  $\nu$  are assumed to be 40 MPa and 0.5, respectively. These values are estimated based on recommendations in the EPRI manual (1990). Using the elastic formulae proposed by Gazetas (1991), the initial stiffness within middle and end regions are  $k_{v\max}^{middle} = 28.2$  MPa/m and  $k_{v\max}^{end} = 263$  MPa/m, respectively. Based on Meyerhof's formula of Eq. (12), the ultimate vertical bearing pressure  $q_{ult}$  is equal to 552 kPa. This value is in good agreement with  $q_{ult} = 549$  kPa obtained from the static vertical push. Following the classical Mohr-Coulomb failure criteria of Eq. (14) with the lowest value of measured undrained shear strength, the ultimate sliding shear strength  $q_{ult}$  is equal to 63 kPa.

The results from correlation studies between experimental and numerical models are presented in Fig. 8 through Fig. 10. Fig. 8 compares the experimental moment-rotation response with the numerical solution obtained with the  $q$ - $z$  contact interface element proposed in this paper. Generally, it is shown that the proposed element can capture well the salient features of the experimental moment-rotation response. These include the moment capacity, stiffness degradation with increasing rotational amplitude, amount of dissipated hysteretic energy, and general shape of hysteretic response. However, the proposed model cannot capture well the initial part of the experimental moment-rotation response. This is due to the inherent drawback of the general hyperbolic function of Eq. 13 in representing the initial part of the soil stress-strain curve. This aspect is worthwhile to investigate further in the future work. The comparison between experimental and numerical settlement-rotation responses is shown in Fig. 9 and confirms that they both show the sinking dominated foundation responses. The evolution of settlement history and the final value of

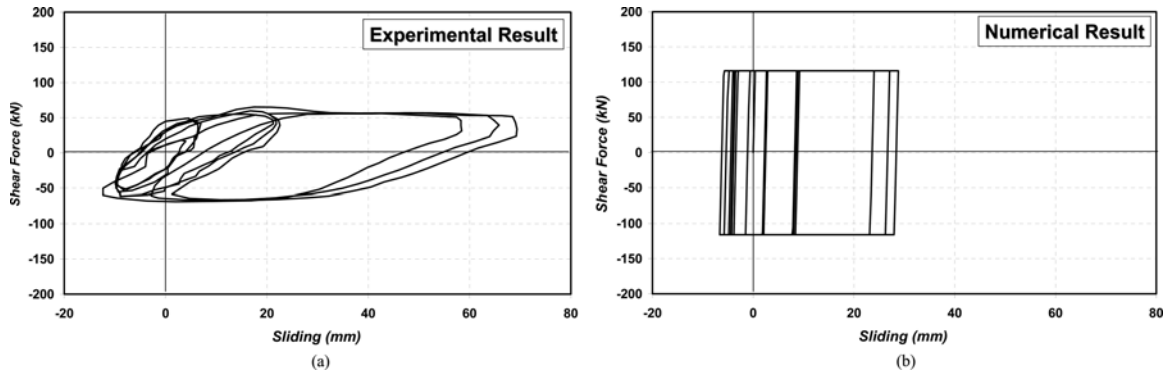


Fig. 10 Experimental and numerical frictional shear-sliding displacement responses of KKR-03 experiment

settlement are predicted well by the proposed model. Since the static vertical factor of safety ( $FS_V \approx 2.8$ ) is relatively small in this test, the accumulated permanent settlement for each loading cycle is clearly observed both in experimental and numerical results. Fig. 10 shows the comparison of experimental result with model simulation for the horizontal shear-sliding displacement response. As opposed to the comparisons in Figs. 8 and 9, the proposed  $t$ - $x$  contact interface element poorly simulates the experimental result. The ultimate sliding shear strength is over-predicted by almost two times while the maximum sliding displacement is under-predicted by almost four times. These discrepancies between experimental and numerical results are mainly caused by the uncoupling response between the vertical bearing pressure and horizontal sliding shear as well as a large value of initial stiffness used to emulate the rigid-plastic behavior. However, the positive aspect of this comparison is that the amount of dissipated hysteretic energy is moderately well predicted by the numerical model.

### 5.2. TRISEE 1-g Experiment: HD test

Large scale experiments on a shallow foundation subjected to static vertical, lateral cyclic, and dynamic loadings were performed at the ELSA laboratory in Italy. This program was funded by the European Commission (EC) under the research project TRISEE (3D site Effects of Soil-Foundation Interaction in Earthquake and Vibration Risk Evaluation). As shown in Fig. 11, the test set-up consists of a  $1 \text{ m} \times 1 \text{ m}$  model foundation, a concrete caisson containing saturated sand, and loading and measurement equipments. The model foundation is made of a steel plate with a concrete interface at the bottom face to obtain a high frictional resistance against horizontal movement. The concrete-caisson dimensions are  $4.6 \text{ m} \times 4.6 \text{ m}$  in plan and  $4 \text{ m}$  in height. The sand used in these experiments is the Ticino sand with well-known geotechnical properties (Bellotti *et al.* 1996). Two relative sand densities are used,  $Dr = 85\%$  (high density denoted “HD”) and  $Dr = 45\%$  (low density denoted “LD”). The frictional angles of HD and LD sands are 42 and 38 degrees, respectively. The model foundation is placed  $1 \text{ m}$  below the soil surface to simulate a lateral overburden pressure of approximately  $20 \text{ kPa}$ . A  $1 \text{ m}$ -high steel framework is placed around the model foundation to retain surrounding sand. In this study, the experimental results of the model foundation on high density sand subjected to lateral cyclic loadings are selected to validate the proposed shallow foundation model. More details of the experiments can be found in the research report by Negro *et al.* (1998).

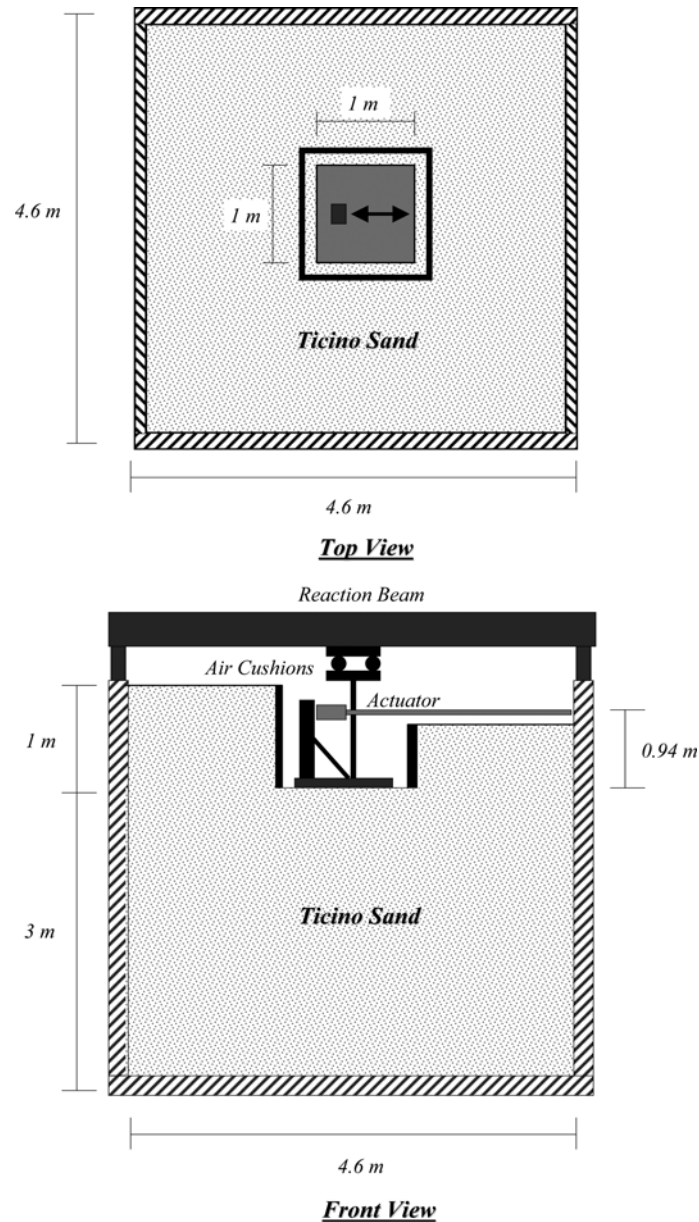


Fig. 11 Test setup of TRISEE experiment (After Negro *et al.* 1998)

As shown in Fig. 11, an air cushion system is used to transmit the constant vertical load of 300 kN during the test. Using Meyerhof's formula of Eq. (12), this value of vertical load results in a static vertical factor of safety  $FS_V \approx 12.5$ . However, this value of  $FS_V$  is much higher than that reported by several researchers (Negro *et al.* 2000, Faccioli *et al.* 2001, Kutler *et al.* 2003, Gajan 2006, Allotey and El Naggar 2008). They all agree that the appropriate value of  $FS_V$  should be around 5. This discrepancy may be attributed to the overestimation of the surcharge contribution to the ultimate bearing capacity (Cernica 1995). After the static vertical push, three phases of lateral

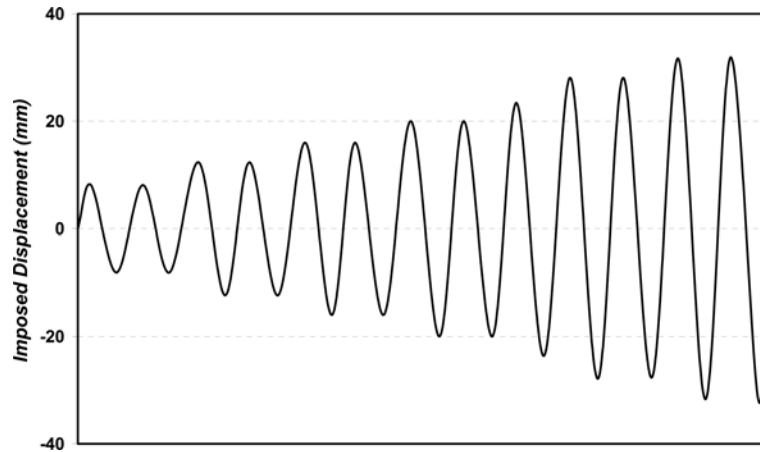


Fig. 12 Imposed displacement history of TRISEE HD Sand experiment

cyclic loadings are applied consecutively through an actuator located at 0.94 m above the foundation. During Phase I, a series of small force-controlled amplitudes are applied. During Phase II, the foundation model is subjected to an earthquake-like time history of the base shear obtained from the test on a four-storey reinforced concrete building by Negro *et al.* (1996). During Phase III, sinusoidal displacement cycles of increasing amplitude (Fig. 12) are applied to the top of the structure.

The numerical model previously used in the KKR-03 correlation study is employed here to idealize the sand-foundation-structure system. Following recommendations in the EPRI manual (1990), the elastic modulus  $E$  and Poisson ratio  $\nu$  are 79 MPa and 0.37, respectively. Using the elastic formulae proposed by Gazetas (1991), the initial stiffness within the middle and end regions are  $k_{vmax}^{middle} = 33.4$  MPa/m and  $k_{vmax}^{end} = 311.2$  MPa/m, respectively. Based on the more realistic value of the vertical factor of safety ( $FS_V \approx 5$ ), the ultimate vertical bearing pressure  $q_{ult}$  is estimated to be 1500 kPa. Using the classical Mohr-Coulomb failure criteria of Eq. (14) with  $\delta = 2\phi/3 = 28^\circ$ , the ultimate sliding shear strength  $t_{ult}$  is equal to 160 kPa.

The results from correlation studies between experimental and numerical models are presented in Fig. 13 through Fig. 15. The moment-rotation responses obtained from the experimental and

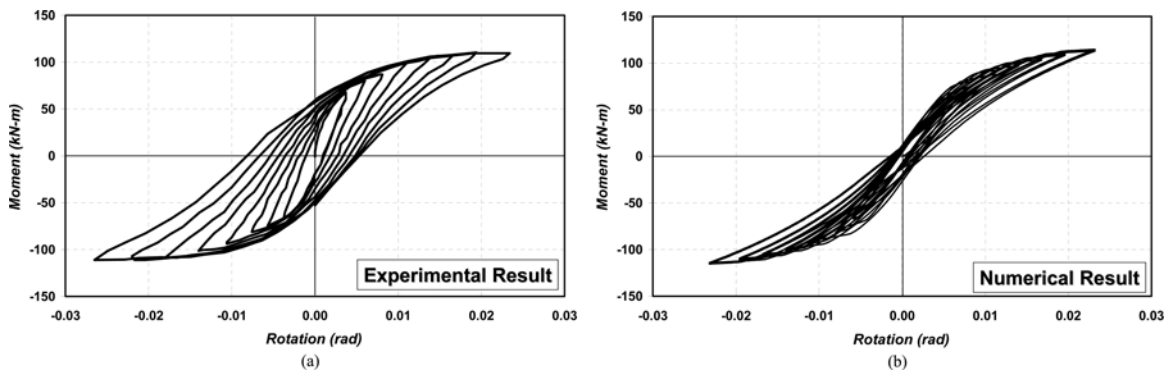


Fig. 13 Experimental and numerical moment-rotation responses of TRISEE HD sand experiment

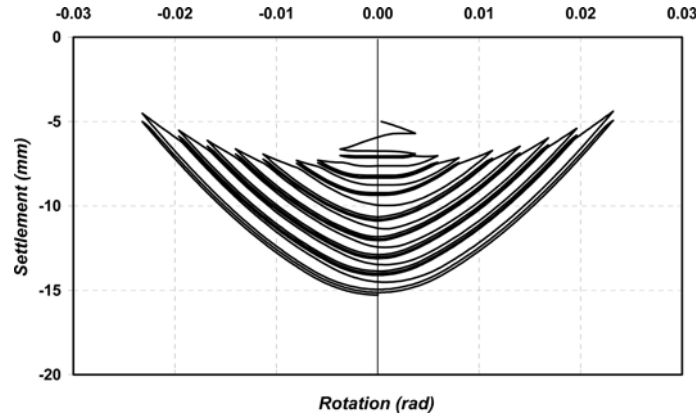


Fig. 14 Numerical settlement-rotation response of TRISEE HD sand experiment

numerical models are compared in Fig. 13. The moment capacity is well predicted by the numerical model while an amount of dissipated hysteretic energy is underestimated. It seems that the gap formed between the sand and the footing during the uplifting mechanism is closed and opened too early. A more refined gap closing-opening model may be required to overcome this discrepancy. Furthermore, inclusion of sand suction strength (tensile strength) may help to delay the gap closing-opening process, hence resulting in a larger amount of dissipated hysteretic energy. However, general features of the experimental moment-rotation response are captured well by the proposed numerical model within acceptable engineering tolerance. The proposed model shows its ability to represent the *S*-shaped moment-rotation response, which is the signature of the uplifting dominated foundation response. This is characteristic of a relatively high value of vertical safety ( $FS_V \approx 5$ ). The rotational stiffness is degraded with increasing rotational amplitude as also observed in the experimental result. Fig. 14 shows the numerical settlement-rotation response. The uplifting dominated foundation response is manifested by the *U*-shaped settlement-rotation response. The accumulation of permanent settlement for each loading cycle can be observed but it is not as severe as in the case of KKR-03 experiment (the sinking dominated response). The proposed model can

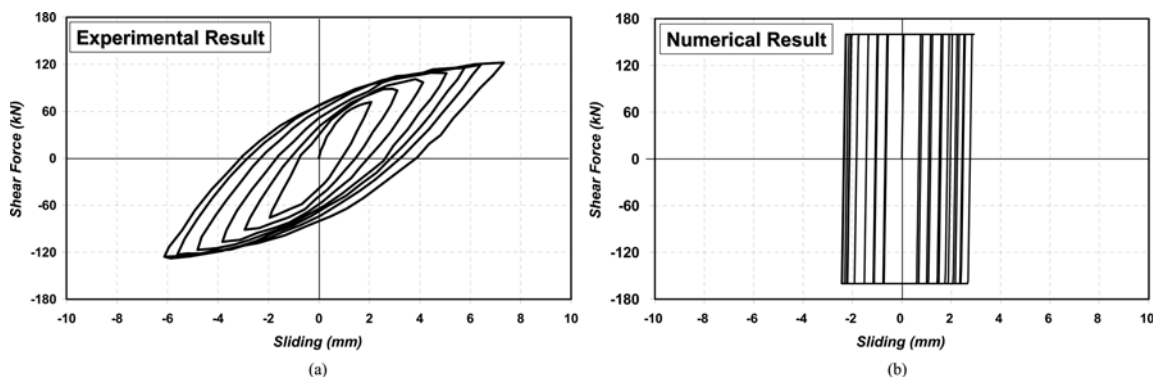


Fig. 15 Experimental and numerical frictional shear-sliding displacement responses of TRISEE HD sand experiment

predict reasonably well the final value of settlement (20 mm for the experiment and 15.3 mm for the simulation). Fig. 15 shows the comparison of experimental result with model simulation for the horizontal shear-sliding displacement response. The ultimate sliding shear strength is slightly over-predicted by the numerical model while the maximum sliding displacement is under-predicted by almost two times. As reasoned earlier, these discrepancies between experimental and numerical results are mainly attributed to the uncoupling response between the vertical bearing pressure and horizontal sliding shear as well as a large value of initial stiffness used to emulate the rigid-plastic behavior. However, the positive aspect of this comparison is that the amount of dissipated hysteretic energy is well predicted by the numerical model.

## 6. Summary and conclusions

This paper presents a simplified but efficient contact interface element for modeling a soil-shallow foundation system. The contact interface sectional response is derived based on fiber section discretization. A general hyperbolic function is used to characterize the stress-deformation relation of each soil fiber. The proposed element can be implemented in a general-purpose structural analysis platform with ease and does not require a high level of user knowledge. The model inputs are based on the general geotechnical soil properties. The soil-foundation interaction mechanisms (sliding, settling, and rocking) are reasonably well represented by the proposed element. The element accuracy is thoroughly assessed against several experimental studies including centrifuge-scale as well as large-scale experiments. For the sinking-dominated foundation (UC-Davis experiment), the proposed element is successful in representing the moment capacity, general shape of hysteretic moment-rotation response, and settlement-rotation evolution. For the rocking-dominated foundation (TRISEE experiment), the proposed element shows its ability to predict the moment capacity and characterize the *S*-shaped moment-rotation as well as *U*-shaped settlement-rotation responses while an amount of dissipated hysteretic energy is underestimated. A more refined gap closing-opening scheme is deemed necessary in correctly predicting the dissipated hysteretic energy in this case. For both foundation types, the model consistently overestimates the ultimate sliding shear strength and underestimates the maximum sliding displacement. This is probably attributed to the uncoupling response between the vertical bearing pressure and horizontal sliding shear as well as a large value of initial stiffness used to emulate the rigid-plastic behavior. However, the amounts of hysteretic energy dissipation are reasonably well predicted in both cases.

The development of the proposed shallow foundation element is a step forward in establishing a computational framework that permits full nonlinear static and dynamic analyses of frame structures including the soil-shallow foundation interaction effects. Both beneficial and detrimental effects due to this interaction mechanism are necessarily accounted for in the numerical model. Consequently, the development of the nonlinear shallow foundation element is an important step toward implementation of the newly proposed Performance-Based Seismic Design and Assessment Methodology.

## Acknowledgements

This study was partially supported by the Thai Ministry of University Affairs (MUA), by the Thailand Research Fund (TRF) under Grant MRG4680109 and Grant RSA5480001, by STREAM

Research Group under Grant ENG-51-2-7-11-022-S, Faculty of Engineering, Prince of Songkla University, by the National Research Foundation of Korea (NRF) grant, and by the Korea government (MEST) under Grant No. 2012-0001556.

## References

- ATC-40 (1996), *Seismic Evaluation and Retrofit of Concrete Buildings*, Applied Technology Council, Redwood City, California.
- Bellotti, R., Jamiolkowski, M., Lo Presti, D. and O'Neil, D. (1996), "Anisotropy of small strain stiffness in Ticino sand", *Geotechnique*, **46**(1), 115-131.
- Burnier, A.A.L., Oliveira, R.R.V., Azevedo, R.F., Azevedo, I.D. and Nogueira, C.L. (2007), "Finite element analysis of a footing load test", *Proceedings of Applications of Computational Mechanics in Geotechnical Engineering*, Guimaraes, Portugal.
- Chatzigogos, C.T., Figini, R., Pecker, A. and Salencon, J. (2011), "A macro-element formulation for shallow foundations on cohesive and frictional soils", *Int. J. Num. Anal. Meth. Geomech.*, **35**(8), 902-935.
- Chopra, A.K. and Yim, C.S. (1985), "Simplified earthquake analysis of structures with foundation uplift", *J. Struct. Div. - ASCE*, **111**(4), 906-930.
- Cernica, J.N. (1995), *Foundation Design*, John Wiley & Sons Inc., New York.
- Cremer, C., Pecker, A. and Davenne, L. (2001), "Cyclic macro-element of soil-structure interaction: material and geometric nonlinearities", *Int. J. Num. Anal. Meth. Geomech.*, **25**(13), 1257-1284.
- Duncan, J.M. and Chang, C.Y. (1970), "Nonlinear analysis of stress and strain in soils", *J. Soil Mech. Found. Div. - ASCE*, **96**(5), 1629-1653.
- Duncan, J.M. and Mokwa, R.L. (2001), "Passive earth pressure: theories and tests", *J. Geotech. Geoenviron. Eng. - ASCE*, **127**(3), 248-257.
- EPRI (1990), *Manual on Estimating Soil Properties for Foundation Design*, Electric Power Research Institute, Palo Alto, California.
- Faccioli, E., Paolucci, R. and Vivero, G. (2001), "Investigation of seismic soil-footing interaction by large scale cyclic tests and analytical models", *Proceedings of 4<sup>th</sup> International Conference on Recent Advances in Geotechnical Earthquake Engineering and Soil Dynamics*, San Diego, California.
- FEMA-273 (1997), *NEHRP Guidelines and Commentary for Seismic Rehabilitation of Buildings*, Washington, DC.
- Gajan, S. (2006), *Physical and Numerical Modeling of Nonlinear Cyclic Load-Deformation Behavior of Shallow Foundations Supporting Rocking Shear Walls*, Doctoral Thesis, Department of Civil and Environmental Engineering, University of California, Davis.
- Gazetas, G. (1991), "Displacement and soil-structure interaction under dynamic and cyclic loadings", *Proceedings of 10<sup>th</sup> European Conference on Soil Mechanics and Foundation Engineering*, Florence, Italy.
- Grange, S., Kotronis, P. and Mazars, J. (2008), "A macro-element for a circular foundation to simulate 3D soil-structure interaction", *Int. J. Num. Anal. Meth. Geomech.*, **32**(10), 1205-1227.
- Hansen, J.B. (1970), "A revised and extended formula for bearing capacity", *Dan. Geotech. Inst. Bull. no. 28*, Copenhagen, Denmark.
- Houlsby, G.T. and Cassidy, M.J. (2002), "A plasticity model for the behavior of footings on sand under combined loading", *Geotechnique*, **52**(2), 117-129.
- Huat, B.B.K. and Mohammed, T.A. (2006), "Finite element study using FE code (PLAXIS) on the geotechnical behavior of shell footings", *J. Comput. Sci.*, **2**(1), 104-108.
- Kutter, B.L., Martin, G., Hutchinson, T.C., Harden, C., Gajan, S. and Phalen, J.D. (2003), "Study of modeling of nonlinear cyclic load-deformation behavior of shallow foundations", *Pacific Earthquake Engineering Research Center Workshop Report*, University of California, Davis.
- Meyerhof, G.C. (1963), "Some recent research on the bearing capacity of foundations", *Can. Geotech. J.*, **1**(1), 16-26.
- Nakaki, D.K. and Hart, G.C. (1987), *Uplifting Response of Structures Subjected to Earthquake Motions*, U.S.-

- Japan Coordinated for Masonry Building Research Report N. 2.1-3.
- Negro, P., Pinto, A.V., Verzeletti, G. and Magonette, G.E. (1996), "PsD test on a four-storey R/C building designed according to Eurocodes", *J. Struct. Eng. - ASCE*, **128**(5), 595-602.
- Negro, P., Verzeletti, G., Molina, J., Pedretti, S., Lo Presti, D. and Pedroni, S. (1998), *Large Scale Geotechnical Experiments on Soil-Foundation Interaction*, Special Publication No. I.98.73, European Commission Joint Research Centre, Ispra, Italy.
- Negro, P., Paolucci, R., Pedretti, S. and Faccioli, E. (2000), "Large scale soil-structure interaction experiments on sand under cyclic load", *Proceedings of 12<sup>th</sup> World Conference on Earthquake Engineering*, Auckland, New Zealand.
- Nova, R. and Montrasio, L. (1991), "Settlements of shallow foundations on sand", *Geotechnique*, **41**(2), 243-256.
- OpenSees (2008), *Open System for Earthquake Engineering Simulation*, Pacific Earthquake Engineering Research Center (PEER), University of California, Berkeley.
- Paolucci, R. (1997), "Simplified evaluation of earthquake-induced permanent displacements of shallow foundations", *J. Earthq. Eng.*, **1**(3), 563-579.
- Potyondy, J.G. (1961), "Skin friction between various soils and construction materials", *Geotechnique*, **11**(1), 243-256.
- Raychowdhury, P. (2008), *Nonlinear Winkler-Based Shallow Foundation Model for Performance Assessment of Seismically Loaded Structures*, Doctoral Thesis, Department of Civil and Environmental Engineering, University of California, San Diego.
- Rosebrook, K.R. (2001), *Moment Loading on Shallow Foundations: Centrifuge Test Data Archives*, Master Thesis, Department of Civil and Environmental Engineering, University of California, Davis.
- Scott, R.F. (1981), *Foundation Analysis*, Prentice-Hall Inc., Eaglewood Cliffs, New Jersey.
- SEAOC (1995), *Vision 2000: Performance Based Seismic Engineering of Buildings*, Structural Engineers Association of California, Sacramento, CA.
- Shirato, M., Paolucci, R., Kuono, R., Nakatani, S., Fukui, J., Nova, R. and di Prisco, C. (2008), "Numerical simulation of model tests of pier-shallow foundation systems subjected to earthquake loads using an elasto-uplift-plastic macro element", *Soils Found.*, **48**(5), 693-711.
- Spacone, E., Filippou, F.C. and Taucer, F.F. (1994), "Fibre beam-column model for nonlinear analysis of R/C frames: part I- formulation", *Earthq. Eng. Struc. Dyn.*, **25**, 711-725.
- Taylor, P.W., Barlett, P.E. and Weissing P.R. (1981), "Foundation rocking under earthquake loading", *Proceedings of 10<sup>th</sup> International Conference on Soil Mechanics and Foundation*, Rotterdam, The Netherlands.
- Taylor, R.L. (2000), *FEAP: A Finite Element Analysis Program. User manual: version 7.3*, Department of Civil and Environmental Engineering, University of California, Berkeley.
- Terzaghi, K. (1943), *Theoretical Soil Mechanics*, Wiley, New York.
- Ugalde, J. (2007), *Centrifuge Test on Bridge Columns on Shallow Square Footings*, Master Thesis, Department of Civil and Environmental Engineering, University of California, Davis.
- Yang, Y.B., Hung, H.H. and He, M.J. (2000), "Sliding and rocking response of rigid blocks due to horizontal excitations", *Struct. Eng. Mech.*, **9**(1), 1-16.